

3-4 Transmission Line Model for Ground Magnetic Disturbances

KIKUCHI Takashi

Many observations have indicated that the magnetospheric convection electric field is transmitted to the low latitude ionosphere and to the inner magnetosphere within several minutes, and cause prompt development of ground magnetic disturbances and of the plasma convection in the global ionosphere and in the inner magnetosphere. One of the purposes of this paper is to review the global features of the ground magnetic disturbances and the 3-dimensional current models explaining the observations. The other purpose is to propose the magnetosphere-ionosphere transmission line model that explains the transmission of the Poynting flux from the outer magnetosphere to the low latitude ionosphere and to the inner magnetosphere.

Keywords

Ground magnetic disturbances, Magnetosphere-ionosphere current system, Magnetosphere-ionosphere convection, Earth-ionosphere waveguide model, Transmission line model

1 Ground Magnetic Disturbances

1.1 Current Systems of Geomagnetic Sudden Commencements and Sudden Impulses (SC/Si)

1.1.1 PRI electric field and current

Geomagnetic sudden commencement (SC) and sudden impulse (Si) are observed on the ground as stepwise increases in the H-component of the geomagnetic field at low latitude (DL). However, in the morning sector in high latitude regions, they appear as positive impulses lasting approximately 1 minute, followed by negative changes lasting from several to tens of minutes (SC(+)). In the afternoon sector at high latitudes, magnetic field disturbances in the opposite direction, SC(-), are observed (Nagata, 1952 ; Matsushita, 1962 ; Araki, 1977). The initial impulse is called the preliminary impulse (PI). The subsequent disturbances in the magnetic field are called the main impulse (MI). In particular, the negative impulse in the high-latitude afternoon sector is called the preliminary reverse impulse (PRI). The PRI is rarely observed at low latitudes, but has been found

to reappear at the dayside magnetic equator (Matsushita, 1962 ; Araki, 1977). Furthermore, the MI at the dayside equator is known to be significantly amplified compared to occurrences at low latitudes (Equatorial enhancement, Sugiura (1953)).

These ground geomagnetic disturbances are caused by 3-D electric current systems flowing in the magnetosphere-ionosphere system. When the magnetosphere is compressed by solar wind shock, the Chapman-Ferraro current on the magnetopause is intensified, which in turn enhances the magnetic field inside the magnetopause. This enhanced magnetic field propagates in the equatorial plane of the magnetosphere as a compressional magnetohydrodynamic (MHD) wave, and results in the DL on the ground. In the immediate interior of the magnetopause, field-aligned currents (FACs) are generated and carry the dusk-to-dawn electric field to the polar ionosphere (Tamao, 1964). This electric field creates a two-cell (DP 2-type) Hall current in the high-latitude ionosphere, which produces the afternoon PRI and the morning reversed PRI (i.e., PPI: preliminary positive impulse). This

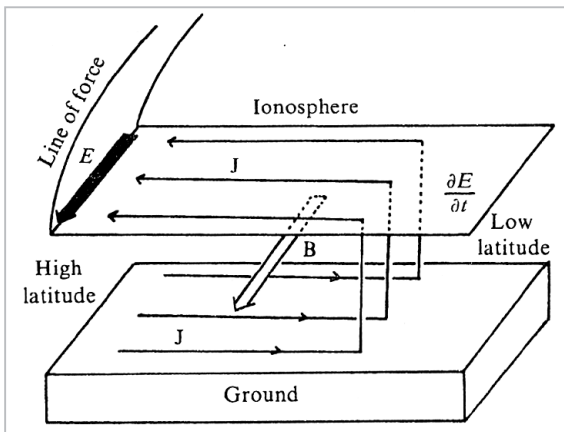


Fig. 1 The Earth-ionosphere-waveguide model (Kikuchi et al., 1978).

The polar electric field is transmitted to low altitudes at the speed of light by TM₀ mode.

electric field is propagated to low latitudes at the speed of light by the TM₀ (0th-order transverse magnetic) mode in the Earth-ionosphere waveguide (Fig.1) (Kikuchi et al., 1978 ; Kikuchi and Araki, 1979).

Since the intensities of electric fields propagated toward low latitudes attenuate geometrically, PRI is rarely observed at low latitudes. However, since the external magnetic field is horizontal in the magnetic equatorial ionosphere, the vertical Hall current induced by the EW electric field produces a vertical polarization electric field, which amplifies the original Pedersen current (Cowling effect: Hirono, 1952). Thus, the PRI, which had disappeared at low latitudes, reappears in the dayside magnetic equator (Araki, 1977 ; Kikuchi et al., 1978).

1.1.2 MI electric field and current

The MI is observed as stepwise increases in the H-component of the magnetic field on the ground (DL). However, in the high-latitude afternoon sector and the dayside magnetic equator, MI amplitude increases, while the magnetic field declines in the high-latitude morning sector (Sugiura, 1953 ; Forbush and Vestine, 1955 ; Obayashi and Jacobs, 1957). The DL is created by the intensified Chapman-Ferraro current in the magnetopause.

Disturbances due to polar ionospheric currents (DP(MI)) displaying latitude and local-time dependencies are generated by the DP 2-

type current system produced by the dawn-to-dusk electric field that results from the compression-driven enhancement of magnetospheric convection (Araki, 1994). Most SC/Si ground magnetic disturbances involve a superposition of the magnetic fields produced by the Chapman-Ferraro current and the PRI and DP(MI) ionospheric currents (Araki, 1977, 1994), but Kikuchi and Araki (1985) found that the onset of SC/Si in mid-latitudes was frequently accompanied by PPI. The PPI could be attributable to positive PI due to PRI ionospheric currents at morning mid-latitudes. But it also occurs in the mid-latitude afternoon sector and near the magnetic equator (Kikuchi and Araki, 1985).

Recently, Kikuchi et al. (2001) analyzed SC accompanying a PRI at the magnetic equator and PPI at the noon mid-latitudes (Fig.2), concluding that it could be explained by magnetic field effects in a 3-D electric current system containing FACs (Fig.3). In other words, instead of the DL due to the Chapman-Ferraro current and the DP(PRI) and DP(MI) ionospheric currents, the dominant factor in creating the mid-latitude PPI is magnetic field effect (according to Biot-Savart's law) directly on the ground of FACs, which are carrying PRI and MI electric fields. They also showed that the afternoon PPI occurrences are distinct in the winter, when the ionospheric current is relatively weak (Kikuchi et al., 2001). The ground magnetic disturbances can be explained by the 3-D current model proposed by Araki (1994) and Kikuchi et al. (2001), which accounts for the effects of the Chapman-Ferraro current, ionospheric current, and the FACs (Fig.3).

1.1.3 HF Doppler Observations

The PRI and MI electric fields that propagate from the polar to the equatorial regions generate ionospheric E region currents, and at the same time, propagate into the ionospheric F region along magnetic field lines to induce plasma motion perpendicular to the magnetic field lines. The method of HF Doppler observations at low latitudes used to observe ionospheric electric fields is based on the Doppler

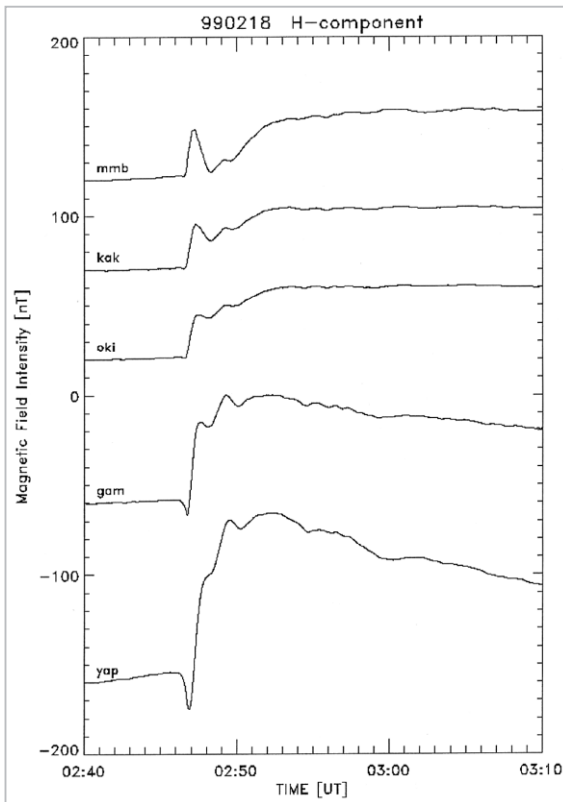


Fig.2 SC accompanying PPI in mid-latitudes (mmb, kak) and PRI at the equator (gam, yap).

The equatorial PRI can be explained by ionospheric currents and the mid-latitude PPI by magnetic field effects of field-aligned currents (Kikuchi et al., 2001).

frequency change exhibited by HF standard radio waves when they are reflected by moving ionospheric F region. Kikuchi et al. (1985) showed that during SC, the HF Doppler frequency deviations (SCF: SC-associated frequency deviation) can be characterized as SCF(+−) during daylight hours and SCF(−+) at night. This day/night reversal of frequency deviation cannot be explained by the westward electric field accompanying the compressional MHD waves that carry the DL component, and should be attributed to the dusk-to-dawn and dawn-to-dusk electric fields that accompany PRI and DP(MI).

Kikuchi (1986) discovered that high-latitude PRI onset in high latitudes occurred simultaneously with SCF(−+) onset at the nightside low latitudes within a temporal resolution of 10 sec. (Fig.4), and proved the instantaneous propagation of the polar electric field to the equator indicated by Araki (1977) by direct observation at low latitudes. Kikuchi (1986) also showed that the positive initial frequency deviations of the dayside SCF(+−) and high-latitude PRI onset occur simultaneously, although this does not pre-

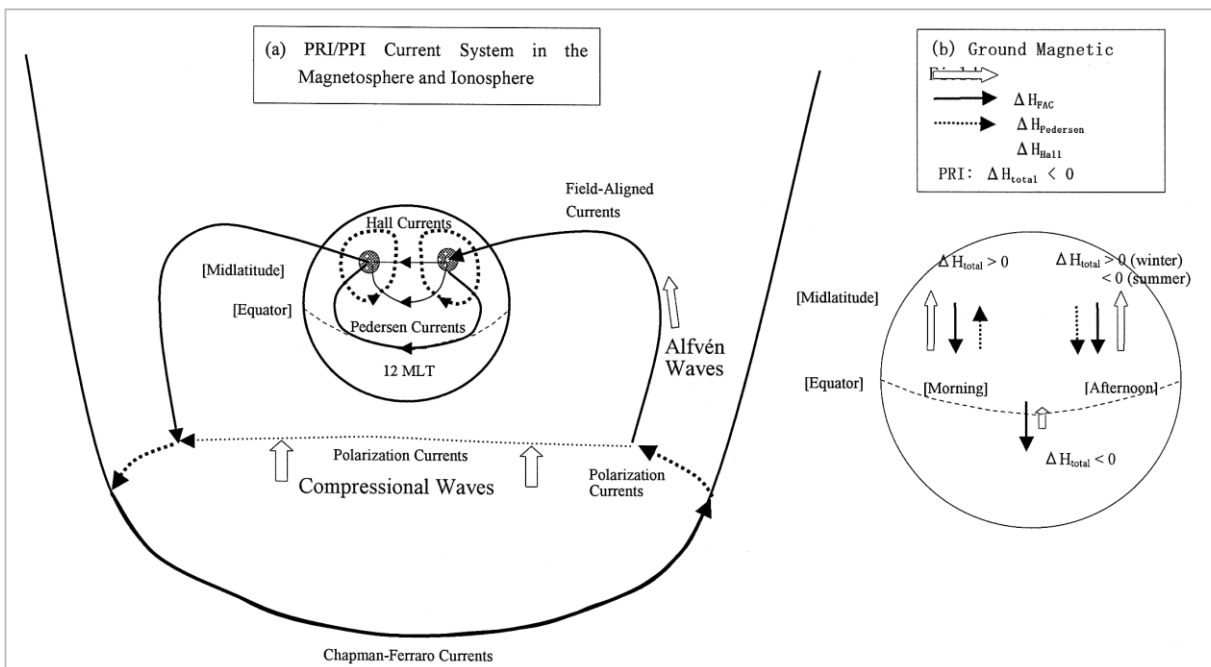


Fig.3 Schematic diagram of the magnetosphere-ionosphere current system of the PRI/PPI of SC.

The PRI/PPI observed from the mid-latitudes to the equator are caused by the 3-D current system composed of field-aligned currents, ionospheric Hall currents, and the ionospheric Pedersen currents (Kikuchi et al., 2001).

clude the possibility of a contribution from the westward electric field associated with compressional MHD waves.

Kikuchi et al. (2002) have performed a quantitative analysis of the equatorial PRI and DP(MI) measured simultaneously with the dayside low-latitude SCF(+/-) on the same meridian (Fig.5). Their results indicate potential contributions from the electric field of the compressional MHD waves to the dayside low-latitude ionosphere.

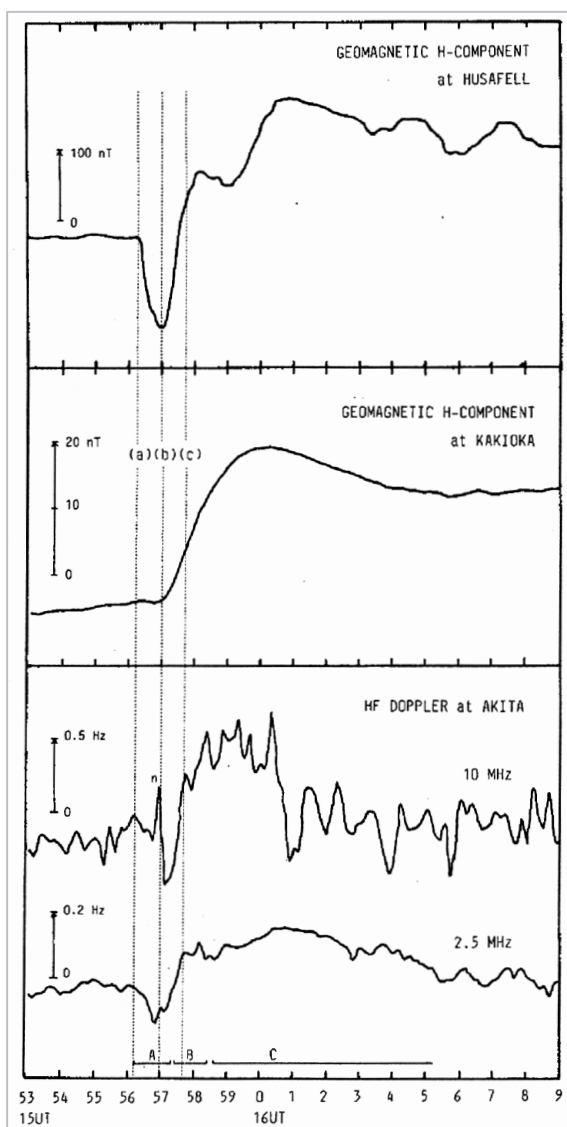


Fig.4 The negative HF Doppler frequency change observed in the midnight middle-to-low latitudes (bottom panel) observed simultaneously with high latitude PRI (top panel), showing the instantaneous propagation of the dusk-to-dawn electric field associated with the PRI to the nightside low latitude ionosphere (Kikuchi, 1986).

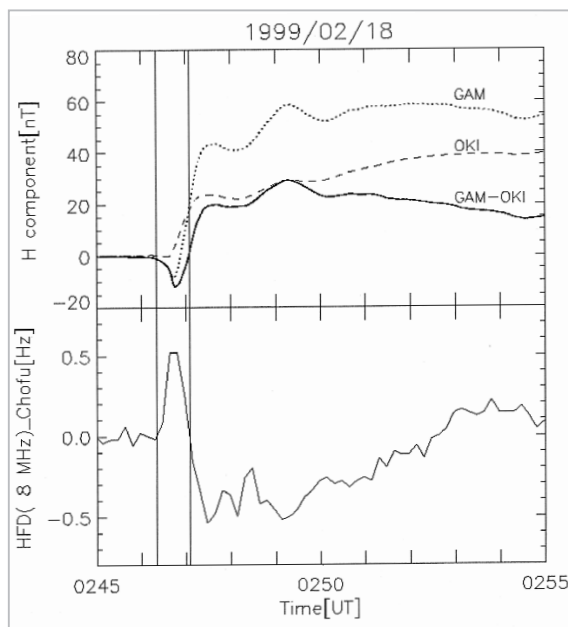


Fig.5 The Positive HF Doppler frequency change observed in the dayside low latitudes (bottom panel) observed simultaneously with the PRI observed at the dayside magnetic equator (GAM)(upper panel).

When the magnetic field component due to the Chapman-Ferraro current (OKI) is subtracted from the dayside magnetic equator PRI (GAM), the resulting ionospheric current component (GAM-OKI) has commencement and peak coinciding with those of the ionospheric electric field with a precision of 10 sec.

1.2 Current System of Geomagnetic Pulsation

PC5-type geomagnetic pulsation (period: 150-600 sec.) is observed mainly in the auroral latitudes. There is a reversal in the rotational direction of its magnetic field vectors at the latitude of maximum amplitude, resulting in an 180° phase difference of vectors on both sides of the latitude (Samson et al., 1971). These properties have traditionally been interpreted in terms of the field line resonance of monochromatic surface waves penetrating into the magnetosphere, induced by Kelvin-Helmholtz instabilities in the magnetopause (Southwood, 1974 ; Chen and Hasegawa, 1974). Kivelson and Southwood (1985) proposed an alternate model of magnetospheric cavity resonance caused by solar wind impulses to explain PC 5 pulsation with multiple discrete periods. However, the finding that the

observed periods were longer than those predicted from the cavity resonance model led to the proposal of a magnetospheric waveguide model based on propagation in the longitudinal direction (Samson, 1992).

It is known that PC 5 geomagnetic pulsation is pronounced at low latitudes and in particular at the dayside magnetic equator. The amplitude of low-latitude PC5 decreases with latitude, although its period shows no latitude-dependency (Ziesolleck and Chamalaun, 1993). In the magnetic equator, PC 5 amplitude is significantly greater than in low latitude regions, showing a strong correlation with high-latitude PC 5 (Reddy et al., 1994 ; Trivedi et al., 1997). Such latitudinal properties are similar to those of SC/Si. Motoba et al. (2002) have shown that some PC 5 can be explained by a DP2-type ionospheric current system in a manner similar to SC/Si.

Motoba et al. (2002) analyzed the correlation between PC 5 pulsations that occurred simultaneously at high latitudes and the magnetic equator, using data of high temporal resolution (3 seconds). They concluded that the

PC 5 occurrences were simultaneous within this temporal resolution (Fig.6). The fact that the equivalent current is of the DP 2-type and the lack of a time lag between PC 5 pulsations in the polar and equatorial regions indicate that, as with SC/Si, FACs are generated by magnetospheric compression caused by forces such as solar wind dynamic pressure, which transport potential electric fields into the polar ionosphere, thereby inducing ionospheric electric currents.

1.3 DP2 (Convection) Current System

1.3.1 DP2 equivalent current system

Nishida et al. (1966) presented a case involving simultaneous observation of a quasi-periodic geomagnetic disturbance (DP 2-type geomagnetic disturbance) with a period of 10 min. to 1 hour in both polar and magnetic equatorial regions, showing that the geomagnetic disturbances are described by two-cell equivalent current systems at high latitudes and zonal currents at the dayside magnetic equator. Since then, Nishida (1968) has found a strong correlation between DP 2 geomagnetic disturbances and the southward component of the solar wind magnetic field, indicating that disturbances in the magnetospheric convection electric field may be the driving factor for DP 2. Nishida (1968) also pointed out that equatorial DP 2 occurred 2 min. after polar DP2, suggesting that the magnetospheric electric field may penetrate into the equatorial ionosphere by propagating along the equatorial plane of the magnetosphere.

Kikuchi et al. (1996) performed an analysis of the correlation between polar and equatorial DP 2 with a period of 40 min., using a combination of magnetic field data with temporal precision of 1 to 10 seconds and data for the polar electric field observed by EISCAT. Their results indicated that the DP 2 ground magnetic disturbances resulted from Hall currents generated by the convection electric field, and that the polar and equatorial DP 2 displayed a positive correlation with a temporal resolution of 25 sec., with a correlation coefficient of 0.9 (Fig.7). These results sup-

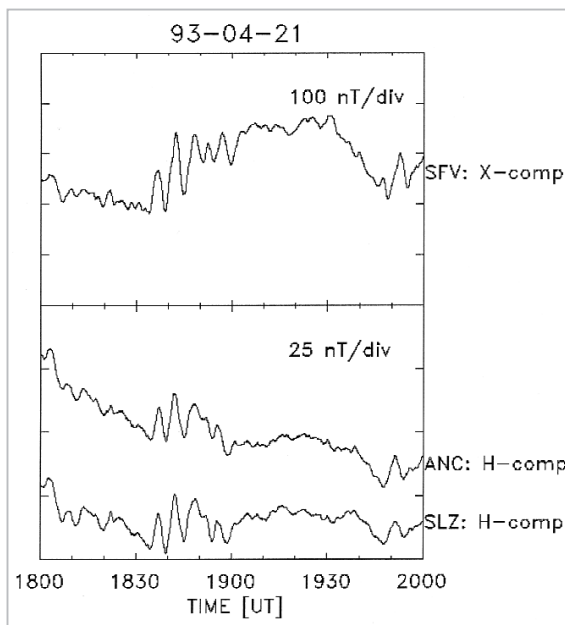


Fig.6 PC5 geomagnetic pulsations observed simultaneously at the magnetic equator and high latitudes, which can be explained by a DP2-type ionospheric current system, similar to SC/Si (Motoba et al., 2002).

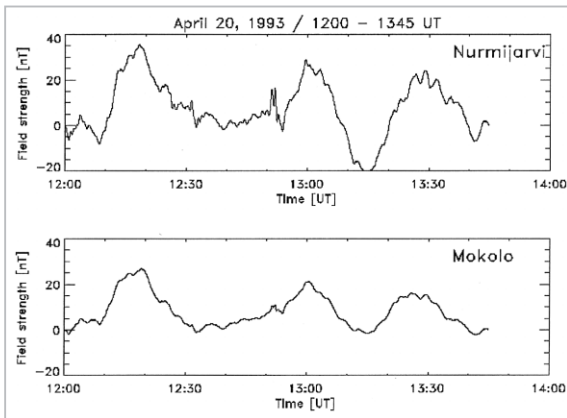


Fig.7 Quasi-periodic geomagnetic field variations (DP2) observed simultaneously at high latitudes (top) and at the magnetic equator (bottom) with a precision of 25 sec, showing near-instantaneous propagation of the polar convection electric field to the equator.

port the near-instantaneous propagation of the convection electric field from the polar to the equatorial ionosphere, similar to SC/Si. It has been shown that the Earth-ionosphere waveguide model proposed for SC/Si (Kikuchi et al., 1978 ; Kikuchi and Araki, 1979) can also be adduced to explain the mechanism of this propagation. In terms of electric current, the

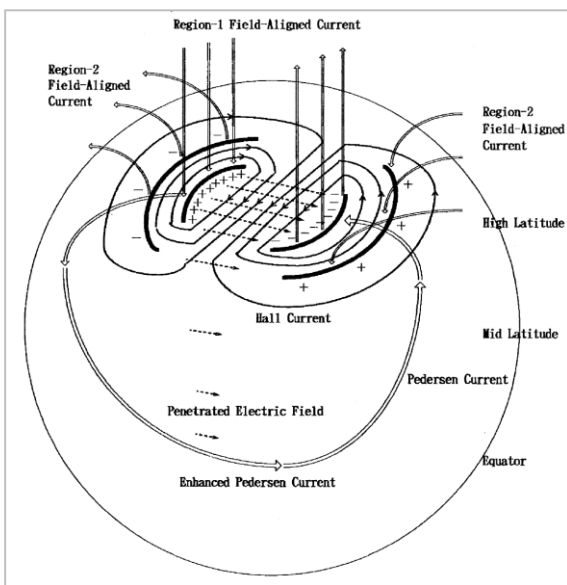


Fig.8 The magnetosphere-ionosphere electric current system that accounts for the DP2 magnetic field variations in the dayside magnetic equator.

The Region-1 field-aligned currents flow into the magnetic equatorial ionosphere via high latitude ionosphere and generate the equatorial DP2 (Kikuchi et al., 1996).

Hall current in high latitudes is induced by the dawn-to-dusk electric field carried in by the region 1 field-aligned currents (R1 FACs) (Iijima and Potemra, 1976), which flows in from the dynamo generated near the magnetospheric cusp to the polar ionosphere (Tanaka, 1995). The R1 FACs also enters the ionosphere as Pedersen currents (Fig.8). The strong DP 2 currents that flow along the magnetic equator connect with the R1 FACs and form the 3-D electric current system that joins with the dynamo in the cusp (Fig.8).

1.3.2 Substorm growth phase

The DP 2 electric fields are also known to develop during the substorm growth phase (Clauer and Kamide, 1985). Kikuchi et al. (2000 a) found that when the substorm growth phase initiates with the southward turning of the IMF, an eastward electrojet in the afternoon auroral belt and an intensification of the magnetic field, corresponding to the convection electric field development from the mid-latitudes to the magnetic equator, were observed to develop simultaneously with a temporal precision of 1 min. (Fig.9). This indicates that at the ionospheric level, the magnetospheric electric field develops almost instantaneously from the polar cap to the magnetic equator in response to the sudden southward turning of the IMF. Kikuchi et al. (2000 a) also found that the sunward plasma flow in the auroral ionosphere develops simultaneously with anti-sunward flow in the polar cap region. This implies that the divergent potential electric field carried in by the R 1 FACs propagates instantaneously.

1.4 DP1 (Substorm) Current System

The structure of the electric field in the mid-to-low latitudes of the ionosphere during substorms is extremely complex, due to the shielding effects of the developing region 2 FACs that form in the inner magnetosphere (Vasyliunas, 1972 ; Crooker and Siscoe, 1981). During the gradual expansion of the convection electric field, a shielding electric field develops and cancels out the convection electric field at low latitudes.

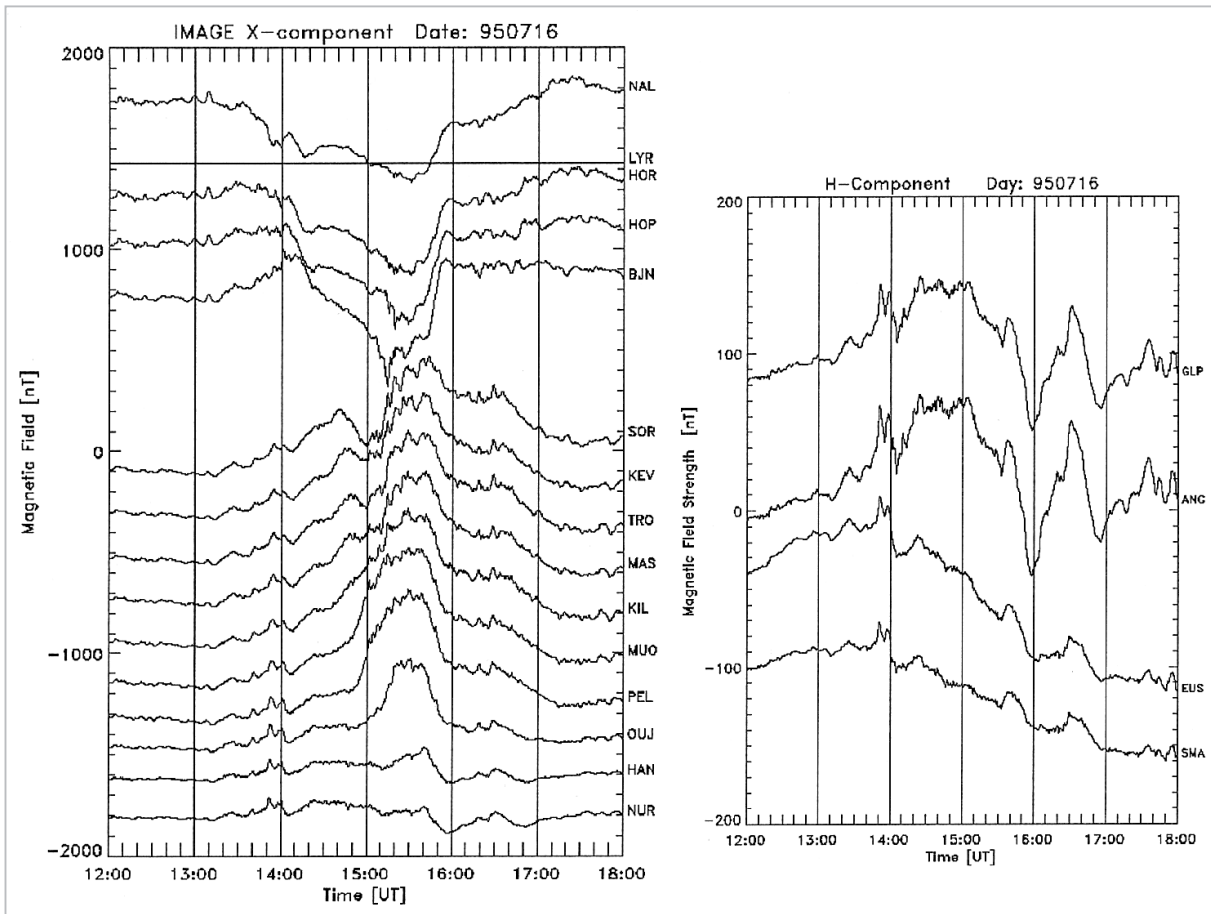


Fig.9 Magnetic field variations in the polar cap to mid-latitudes (left) and at the magnetic equator (right) during a substorm.

The growth phase occurred simultaneously in the polar cap (NAL), auroral belt (TRO), and the mid-latitudes (NUR) at 1313 UT, demonstrating that the global ionospheric current was driven by the magnetospheric convection electric field (Kikuchi et al., 2000a).

The shielding effect is significant at this stage. But when the convection electric field begins to rapidly weaken after the shielding electric field has grown sufficiently strong, the time lag in the attenuation of the shielding electric field leads to a state known as overshielding. In this state, an electric field with direction opposite to the convection electric field is observed in the mid-to-low latitude regions.

Gonzales et al. (1979) found that the electric field observed by the Jicamarca incoherent scatter radar at the equator displayed a rapid weakening in response to the northward turning of the IMF. This corresponds to the overshielding. The rapid reduction of the convection electric field with the northward turning of the IMF is believed to cause overshielding. On the other hand, Kikuchi et al. (2002 b)

observed that the amplitude of the negative bay, which develops in the afternoon low latitude regions during substorms, increases significantly on the magnetic equator. This equatorial amplification of the negative bay was interpreted as resulting from the overshielding effect created by the rapid decrease in the polar electric field observed by EISCAT. They also quantitatively extracted the components of the convection and shielding electric fields from a combination of EISCAT and magnetometer chain data (Fig.10). Their results show that the shielding electric field begins to grow rapidly from substorm onset, and continues to do so even after the convection electric field starts to rapidly decline near the negative bay maximum, leading to the dominance of the shielding electric field over the convection electric field.

In terms of the current system, this can be interpreted as the inflow of R 1 FAC, which drives the convection electric field, as well as R 2 FAC, which creates the shielding electric field, into the equatorial ionosphere (Fig.11). The example of analysis by Kikuchi et al. (2000 b) accompanies a time lag of 17 minutes in the development of the R 2 FAC. For this reason, during the growth phase, the current system formed by the R 1 FAC is dominant, and therefore the eastward electric current is dominant in the equator. In contrast, during the decay phase of the convection electric field, the current system formed by the R 2 FAC dominates, as a result of which the westward electric current becomes dominant at the equator, leading to the weakening of the magnetic field. This results in the amplification of the negative bay at the equator.

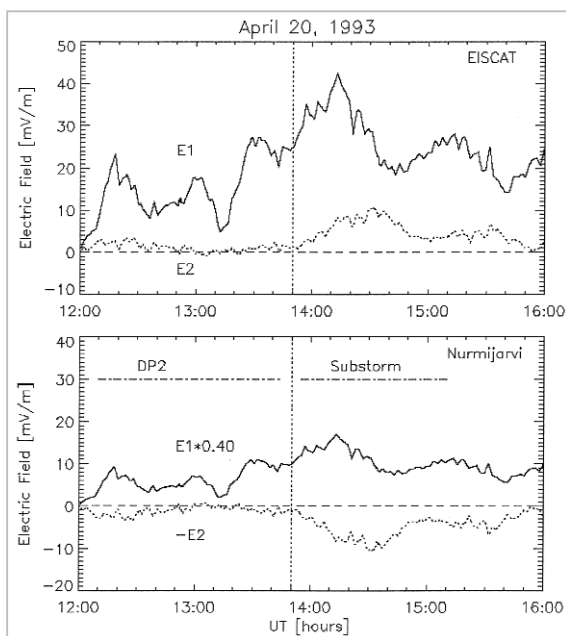


Fig. 10 Convection electric field (E1: solid lines) and shielding electric field (E2: dotted line) at the auroral latitude (top) and mid-latitudes (bottom) determined from electric field observed by EISCAT and magnetometer chain data during DP2 and substorm.

The convection electric field is dominant during the DP2, and the shielding electric field grows during the substorm. During the maximum phase of the substorm, the shielding electric field is dominant in the mid-latitudes (Kikuchi et al., 2000b).

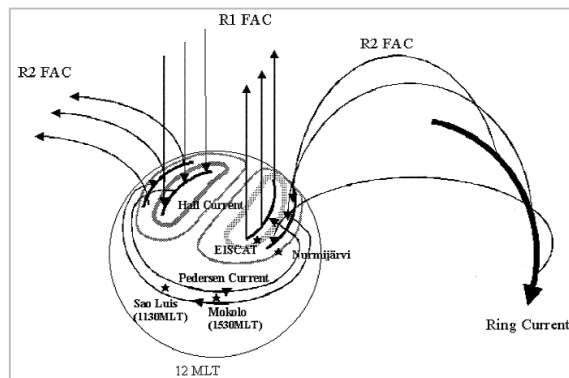


Fig. 11 Magnetosphere-ionosphere current system that develops during the substorm.

The R 1 FAC and R 2 FAC flow from the magnetosphere into the equatorial ionosphere via the polar ionosphere. The R 1 FAC is dominant during the growth phase, and R 2 FAC is dominant around the peak of the substorm (Kikuchi et al., 1996).

1.4.1 Equatorial CEJ

The equatorial counter-electrojet (CEJ) has been described in reports as a phenomenon in which the dayside magnetic field intensity is lower than nightside intensity (Gouin, 1962 ; Hutton and Oyinloye, 1970). The behavior of CEJ in quiet periods has been explained by the ionospheric dynamo resulting from atmospheric tidal motion (Rastogi, 1974). However, Fejer et al. (1976) have pointed out that the counter electric field observed by the Jicamarca radar appeared to correlate with disturbances in the high-latitude electric fields.

Kikuchi et al. (2000 b) reported that the equatorial enhancement of the negative bay due to overshielding during substorms manifests itself as equatorial CEJ. Others have reported that overshielding occurs with the sudden northward turning of the IMF (Kelley et al., 1979 ; Gonzales et al., 1983). Based on an analysis of two equatorial CEJ events resulting from the northward turning of IMF, Kikuchi et al. (2003) proposed a scenario in which equatorial CEJ is caused by the penetration of R 2 FACs into the equatorial ionosphere. In this scenario, after sufficient development of the magnetosphere-ionosphere convection during southward IMF, the IMF turns suddenly northward, causing a rapid decrease in polar electric potential. This triggers the

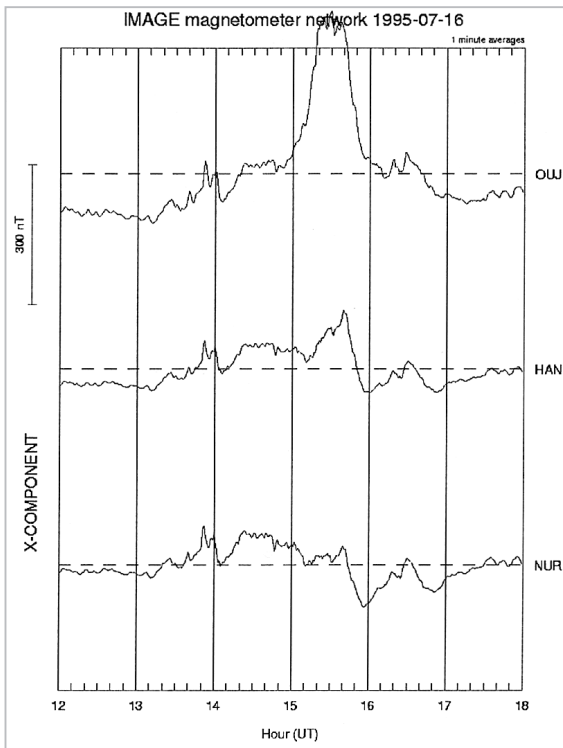


Fig. 12 Magnetic field variations at the auroral to mid-latitudes during a substorm. The weakening in convection electric field at 1543 UT results in the decrease in the eastward auroral electrojet, while a westward current is intensified in the mid-latitudes.

weakening of the fully-developed auroral electrojet current, which is weakened below levels at the start of convection development at mid-latitudes (Fig.12). In short, counter-currents are created in the mid-latitudes. Under these conditions, a strong counter-current is induced in the magnetic equator, creating the equatorial CEJ.

Fig.13 is a schematic diagram of the electric current system due to the dominant R 2 FAC. Note that the counter-current in the mid-latitudes is not a return current of the auroral eastward electrojet, but occurs because the Hall current created by the divergent electric field near the R 2 FACs exceeds the Hall current surrounding the R 1 FAC.

2 The Magnetosphere-Ionosphere Transmission Line Model

As stated in the above sections, geomagnetic disturbances that appear simultaneously

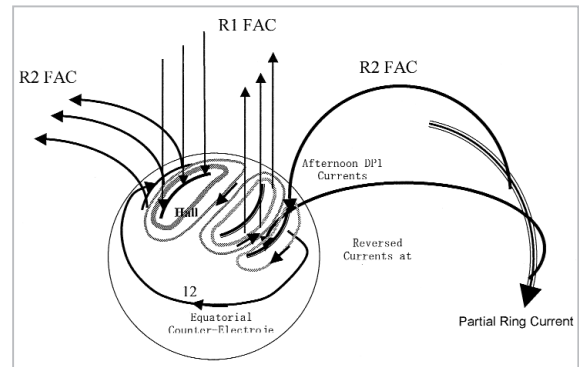


Fig. 13 The mid-latitude and equatorial counter-electrojets that develop during a substorm. The weakening of R1 FAC leads to relative strengthening and dominance of the R2 FAC.

in polar and equatorial regions can be explained in terms of a current system that flows from the polar ionosphere to the equatorial ionosphere. Kikuchi et al. (1978) and Kikuchi and Araki (1979) have proposed a model in which the ionospheric current and the accompanying electric field are propagated from the polar region to the equator by the TM0 mode of the Earth-ionosphere waveguide.

This section proposes a magnetosphere-ionosphere transmission line model coupled with the Earth-ionosphere waveguide, adopting transmission lines instead of FACs as the mechanism propagating convection energy generated in the magnetosphere to the polar ionosphere and the global ionosphere. The magnetosphere-ionosphere transmission line model consists of the following 3 transmission lines: (1) the transmission line that transports energy from the magnetospheric generator to the polar ionosphere; (2) the Earth-ionosphere waveguide (TM0 mode) that transports energy from the polar ionosphere to the low-latitude ionosphere; and (3) the transmission line that transports the ionospheric electric field to the ionospheric F region and the inner magnetosphere. This section also examines a coupled transmission line composed of (1) and (2) as the mechanism responsible for the excitation of the TM0 mode of the Earth-ionosphere waveguide by magnetospheric transmission

lines.

The following section first introduces the detailed properties of the transmission lines that connect the generator and the ionosphere (closed transmission line) in (1), then discusses an initially-charged transmission line in which an initial charge is applied to the transmission line instead of the generator. This model is applied to the Dungey's model, in which magnetic flux transfer event (FTE) is regarded as the driving mechanism for the magnetospheric convection, corresponding to the condition of the whole magnetic flux (= transmission line) having a given velocity at $t = 0$. The Earth-ionosphere waveguide in (2) has been analyzed in detail by Kikuchi and Araki (1979) and will not be discussed here. However, a special case evaluating attenuation of the TM0 mode under the nighttime ionospheric condition will be presented.

Finally, the discussions will address (3), the transmission line that transfers the ionospheric potential difference upwards. When this transmission line is applied to the propagation of the ionospheric electric field to the magnetosphere, the generator of the transmission line corresponds to the ionospheric potential difference, and the ionosphere of the opposite hemisphere becomes the load. But if a north-south hemisphere symmetry is assumed, the currents flowing out of the ionosphere of the two hemispheres mutually cancel on the magnetic equatorial plane. In other words, this case is equivalent to the case of an infinitely large load resistance of the transmission line (open transmission line).

2.1 Generator

Southward IMF promotes magnetic field line reconnection at the front of the magnetosphere, resulting in a coupling between the IMF and the Earth's magnetic field and an anti-sunward movement of magnetic flux. Dungey (1961) proposed a model in which these magnetic flux motions drive large-scale convection in the magnetosphere. On the other hand, a recent MHD simulation (Tanaka, 1995) has shown that the magnetic stress ener-

gy produced by the reconnection generates a region of high plasma pressure on the higher latitude side of the cusp. The electromotive force produced on the tailward side of this high-plasma-pressure region drives R 1 FACs, and induces Pedersen currents in the ionosphere. In this circuit, the electric current on the tailward side of the high-plasma-pressure region corresponds to the generator current, whose Lorentz force is in balance with the plasma pressure gradient. The R 1 FACs can be regarded as transmission lines that transfer magnetospheric plasma convection to the ionosphere and supply the energy consumed by the ionospheric Pedersen current. The electromagnetic energy ($\mathbf{J} \cdot \mathbf{E}$) within the generator is supplied by the kinetic energy of plasma movement in the anti-sunward direction against the Lorentz force ($\mathbf{J} \times \mathbf{B}$), and can be expressed as follows (Iijima, 2000):

$$\mathbf{J} \cdot \mathbf{E} = (\mathbf{J} \times \mathbf{B}) \cdot \mathbf{v} < 0 \quad (1)$$

As evident from the following equation, this energy ($\mathbf{J} \cdot \mathbf{E}$) is the divergence of the Poynting flux $((\mathbf{E} \times \Delta \mathbf{B}_\perp) / \mu_0)$, and represents the release of electromagnetic energy from the generator.

$$\mathbf{J} \cdot \mathbf{E} = -\nabla \cdot (\mathbf{E} \times \Delta \mathbf{B}_\perp) / \mu_0 < 0 \quad (2)$$

This energy is transferred to the ionosphere together with the R 1 FACs, and is converted in the ionosphere into Joule heat $\mathbf{I} \cdot (\mathbf{E} + \mathbf{v}_n \times \mathbf{B}_0)$ and mechanical energy $\mathbf{v}_n \cdot (\mathbf{I} \times \mathbf{B}_0)$, which is transferred to the neutral atmosphere (\mathbf{I} is the altitude-integrated ionospheric current) (Iijima, 2000). Generally, plasma motion is damped within the generator by the Lorentz force due to electric current (the 3 rd term in the equation below). However, the results of simulations by Tanaka (1995) have shown that the contribution from this inertial term is small, and that the plasma pressure and the Lorentz force remain in constant balance.

Therefore, $dV/dt = 0$ in the following equation. Plasma motion does not have to maintain FACs by deceleration, and high-pres-

sure plasma is steadily supplied by the dayside reconnection.

$$\mathbf{J} \times \mathbf{B} - \nabla p - \rho \frac{d\mathbf{V}}{dt} = 0 \quad (3)$$

2.2 Magnetospheric Transmission Lines

The electromagnetic energy released from the generator (Poynting flux) is transferred along magnetic field lines within the space confined by R 1 FACs. This can be explained by the transmission line model. For simplicity, the transmission lines are assumed to consist of parallel planes with width equal to their intervals. This simplified model allows us to discuss the fundamental properties of transmission lines independently of the widths and intervals of FACs. The transmission lines can be represented by a distributed constant circuit with inductance (L), capacitance (C), resistance (R), and conductance (G) per unit length as shown in Fig.14. Given below are the basic equations for this circuit (Cheng, 1963):

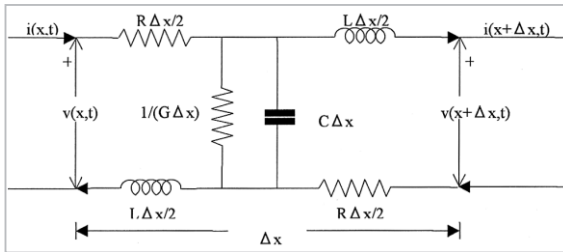


Fig. 14 Basic circuit of the transmission line.

L, R, C, and G, respectively, are inductance, resistance, capacitance, and conductance per unit length.

$$\frac{\partial^2 v}{\partial x^2} = LC \frac{\partial^2 v}{\partial t^2} + (RC + LG) \frac{\partial v}{\partial t} + RGv \quad (4)$$

$$\frac{\partial^2 i}{\partial x^2} = LC \frac{\partial^2 i}{\partial t^2} + (RC + LG) \frac{\partial i}{\partial t} + RGi \quad (5)$$

Here,

v = potential difference

i = electric current

R = resistance per unit length

L = inductance per unit length

G = conductance per unit length

C = capacitance per unit length.

To examine the behavior of the electric potential and currents after the electromotive force is produced at the generator during southward IMF, Laplace transform is applied to the basic equations to solve them as an initial-value problem. The Laplace transform $V(s)$ of $v(t)$ and the inverse Laplace transform can be expressed as follows:

$$V(x, s) = \int_0^{\infty} v(x, t) e^{-st} dt \quad (6)$$

$$v(x, t) = \frac{1}{2\pi j} \int_{\sigma - j\infty}^{\sigma + j\infty} V(x, s) e^{st} dt \quad (7)$$

After Laplace transform, the basic equations are:

$$\frac{d^2 V}{dx^2} - \gamma^2 V = L \frac{di(x, 0)}{dx} - C(Ls + R)v(x, 0) \quad (8)$$

$$\frac{d^2 I}{dx^2} - \gamma^2 I = C \frac{dv(x, 0)}{dx} - L(Cs + G)i(x, 0) \quad (9)$$

$$\gamma = \sqrt{(Ls + R)(Cs + G)} \quad (10)$$

Here, field-aligned resistance R and the conductance across the magnetic field lines are both assumed to be zero. If the electromotive force of the generator is assumed to be a constant E at $t > 0$, the electromotive force can be expressed as $E U(t)$ (where U is the Heaviside step function), and its Laplace transform becomes E/s . When r is the internal resistance of the generator ($x = 0$) and R is the resistance of the ionosphere acting as the load, the potential difference and the current after Laplace transform at distance x from the generator can be expressed as follows:

$$V(x, s) = \frac{E}{s} \frac{R_0}{r + R_0} \frac{e^{-\gamma x} + \Gamma e^{-2\gamma d} e^{\gamma x}}{1 - \Gamma \Gamma' e^{-2\gamma d}} \quad (11)$$

$$I(x, s) = \frac{E}{s} \frac{1}{r + R_0} \frac{e^{-\gamma x} - \Gamma e^{-2\gamma d} e^{\gamma x}}{1 - \Gamma \Gamma' e^{-2\gamma d}} \quad (12)$$

$$\gamma = \sqrt{LC} s = \frac{s}{c} \left(c = \frac{1}{\sqrt{LC}} \right) \quad (13)$$

$$\Gamma = \frac{R_1 - R_0}{R_1 + R_0} \quad (14)$$

$$\Gamma' = \frac{r - R_0}{r + R_0} \quad (15)$$

Here, d is the length of the transmission line (15 Earth radii (R_e)), Γ is the reflection

coefficient of the electric field at the ionosphere, and Γ' is the reflection coefficient at the generator for waves reflected back to the generator by the ionosphere.

Below are the equations for potential difference and current given by the Laplace transform of the above solutions.

$$v(x,t) = E U(t) - E \frac{R_g}{R_1 + R_g} \left\{ \sum_{n=1}^{\infty} \Gamma^{n-1} U\left(t - \frac{(2n-1)d-x}{c}\right) + \sum_{n=1}^{\infty} \Gamma'^{n-1} U\left(t - \frac{(2n-1)d+x}{c}\right) \right\} \quad (18)$$

$$i(x,t) = E \frac{1}{R_1 + R_g} \left\{ \sum_{n=1}^{\infty} \Gamma^{n-1} U\left(t - \frac{(2n-1)d-x}{c}\right) - \sum_{n=1}^{\infty} \Gamma'^{n-1} U\left(t - \frac{(2n-1)d+x}{c}\right) \right\} \quad (19)$$

2.2.1 Closed transmission lines (magnetospheric generator-ionospheric Pedersen conductance)

Here, I will focus on the closed transmission line formed by the transmission line (R 1 FAC) from the generator near the cusp (Tanaka, 1995) and the Pedersen current in the polar ionosphere. For the sake of simplicity, the internal resistance of this generator is assumed to be zero. When the Alfvén velocity of the magnetosphere $V_a = 2,000$ km/s, the characteristic conductance of the MHD medium is given as $\Sigma_A = 0.40$ mho. Fig.15 shows the temporal changes in electric potential difference and current at the generator and the ionosphere when the ionospheric conductance is assumed to be $\Sigma_I = 4\Sigma_A = 1.6$ mho. As in the upper-left panel in Fig.15, the potential difference at the generator was assumed to increase with a stepwise function. The upper-right panel in Fig.15 shows that the potential difference at the ionosphere asymptotically approaches that of the generator with a relaxation time of 5-10 minutes. The current (middle panel) and energy (bottom panel) of both the generator and ionosphere asymptotically approach a steady state. This relaxation time can be understood as follows: The potential difference produced at the generator propagates at the Alfvén velocity and is reflected by the ionosphere upon arrival. Since the coefficient of reflection for the potential difference at the ionosphere is -0.6 , the amplitude of the reflected wave should be -0.6 for an incidence potential difference of 1. The composite potential difference would be 0.4 at the

ionosphere, corresponding to the initial amplitude in the ionospheric potential difference shown in the upper-right panel in Fig.15. With the upward propagation of the reflected wave, the wave with composite amplitude of 0.4 should move upward. However, the actual wave component that propagates up is the reflected wave with amplitude of -0.6 , considered here to be the primary reflected wave. Since the internal resistance of the generator is zero, the coefficient of reflectance for this primary wave at the generator is -1 , and the secondary reflected wave would have amplitude 0.6. Combined with the upward propagating wave with composite amplitude 0.4, this secondary reflected wave forms a wave with an amplitude of 1. This means that the generator will always maintain an electromotive force with an amplitude of 1. The secondary reflection at the generator propagates downward, and the potential difference with composite amplitude of 1 will arrive again at the ionosphere.

The arrival of the secondary reflected wave with amplitude of 0.6 at the ionosphere would result in a tertiary reflected wave of -0.36 , since the coefficient of reflection is -0.6 . Therefore, the composite potential difference should be 0.64. This corresponds to the second step in the potential difference shown in the upper-right panel of Fig.15. Repeating such reflections between the ionosphere and the generator makes it possible to increase the potential difference at the ionosphere in steps, while keeping the potential difference at the generator constant at 1. The length of the transmission line is assumed to be 15 Re. Since the Alfvén velocity is 2,000 km/s, the propagation time from the generator to the ionosphere is 48 seconds. Therefore, the first step of the increase in the potential difference at the ionosphere in Fig.14 occurs 48 seconds after the increase at the generator; the second step occurs 96 seconds later. Assuming the internal resistance of the generator to be zero means that the generator is capable of recovering the potential difference lost due to the reflection at the ionosphere to the original

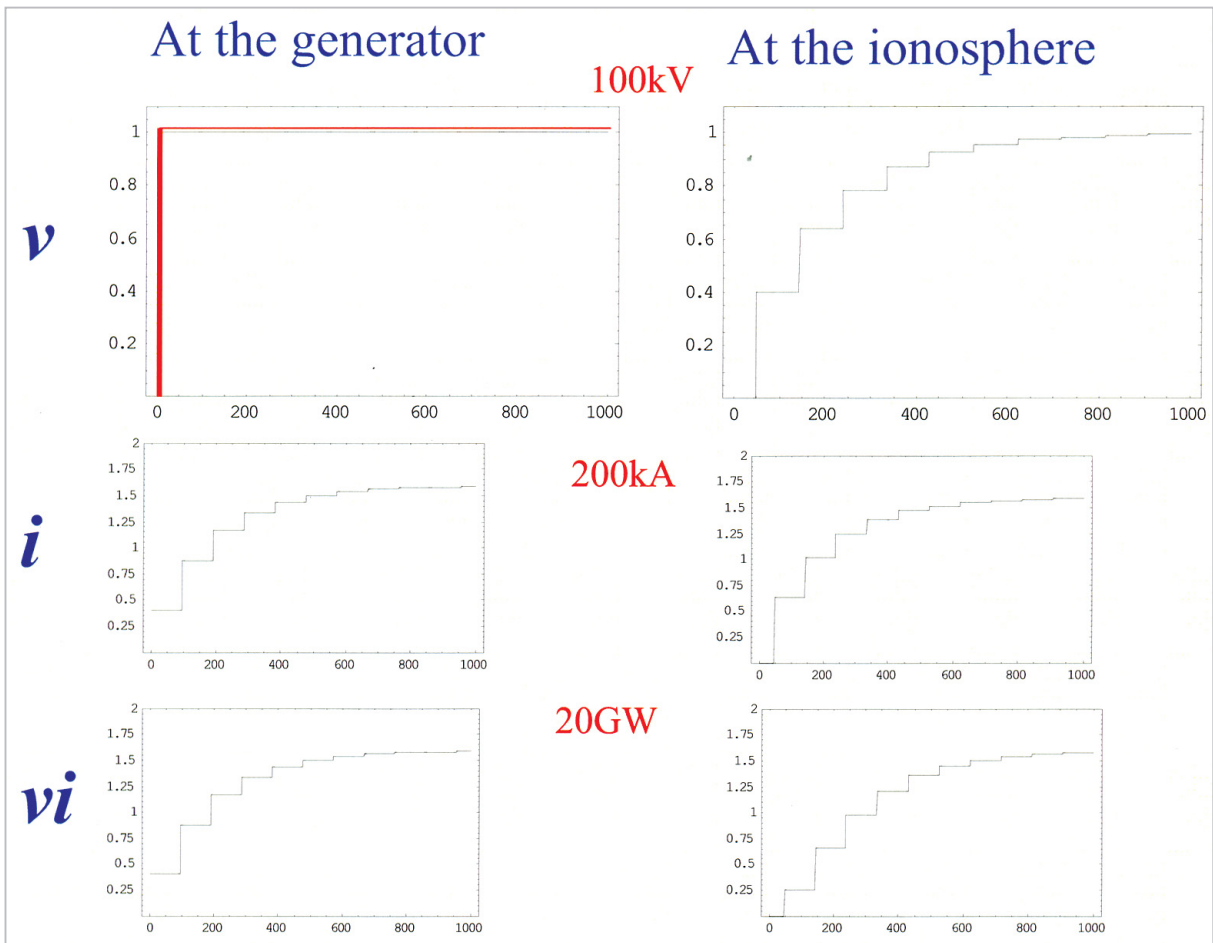


Fig. 15 The electric potential (upper left), current (middle left), and energy (lower left) at the generator, and the electric potential (upper right), current (middle right), and energy (lower right) at the ionosphere, assuming that the internal resistance of the generator = 0, $V_a = 2,000$ km/s, and ionospheric conductance = 1.6 mho in the magnetosphere-ionosphere transmission line model.

For clarity, the values for current and energy are calculated on the assumption that the electric potential difference of 1 is equivalent to 100 kV.

value. As evident from Eq. (3) which represents the balance of force within the generator, maintaining a constant potential difference is equivalent to maintaining constant plasma velocity, allowing us to ignore the inertial term in the equation.

The balance achieved between the Lorentz force due to the generator current and the plasma pressure in Tanaka's (1995) results signifies a generator with internal resistance of zero.

2.2.2 Initially-Charged Transmission Line (FTE-Ionospheric Pedersen Conductance)

Dungey's (1961) model, which states that the anti-sunward movement of the magnetic flux generated by the reconnection between

the Earth's magnetic field and the solar wind magnetic field drives the magnetospheric convection, is widely accepted. According to this model, the solar wind electric field penetrates into the magnetosphere along magnetic field lines and sustains plasma motion. This solar wind electric field pulls on the magnetized plasma in the ionosphere and drives ionospheric convection (see, for example, Cowley and Lockwood, 1992).

Regardless of the processes in the magnetosphere, ionospheric plasma motion is always accompanied by an electric field in the ionosphere. Since the ionospheric electric field also induces Pedersen currents in the conductive ionosphere, energy is lost. This energy loss is thought to damp the motions of the

FTE within the magnetosphere and reduce initial velocity.

The equation of motion (3) in the previous section contains no pressure term. Convection is sustained by the balance between the Lorentz force due to the generator current and the inertial force. The initial velocity imparted to the magnetic flux as a result of reconnection is equivalent to providing an initial potential difference to the transmission line.

In the transmission line model of the previous section, substituting the transmission lines with ones with the generator located at the open end ($r = \infty$) and assigning an initial potential difference of E to the whole transmission line is equivalent to assigning an initial velocity of E/B to the magnetic flux in the magnetosphere.

The following calculations assume that the length of the transmission lines is $15 R_E$. But if the magnetic field lines are assumed to be open in the solar wind, as in Dungey's model, the length will be even longer. The initial potential difference propagates into the ionosphere, the reflected waves damping the potential difference while propagating upwards.

Here, the polarization electric current flowing on the surface of the wave propagating in the transmission lines corresponds to the generator current in the previous case. The polarization current moves upward—that is, into the solar wind—as it continues to travel along with the movement of the surface of the wave, and causes the magnetic flux in this path to decelerate.

Only the composite potential difference with amplitude of 0.4 resulting from the primary reflection at the ionosphere in Fig.15 is sustained. There is no stepwise increase of the ionospheric potential difference approaching the original potential difference of the generator. When the magnetic flux tube is closed within the magnetosphere, and as long as the source is limited to the inertial current, the repeated reflection will continue only to reduce plasma velocity. Hence, the potential difference in the magnetosphere and iono-

sphere will be attenuated.

When an initial potential difference is assigned to the transmission line, the potential difference and current are obtained as solutions of the following initial-value problems:

$$v(x,t) = EU(t) - E \frac{R_0}{R_1 + R_0} \left\{ \sum_{n=1}^{\infty} \Gamma^{n-1} U\left(t - \frac{(2n-1)d-x}{c}\right) + \sum_{n=1}^{\infty} \Gamma^{n-1} U\left(t - \frac{(2n-1)d+x}{c}\right) \right\} \quad (18)$$

$$i(x,t) = E \frac{1}{R_1 + R_0} \left\{ \sum_{n=1}^{\infty} \Gamma^{n-1} U\left(t - \frac{(2n-1)d-x}{c}\right) - \sum_{n=1}^{\infty} \Gamma^{n-1} U\left(t - \frac{(2n-1)d+x}{c}\right) \right\} \quad (19)$$

Fig.16 shows the results of calculations using the same parameters used in the previous section. Not only is the ionospheric potential difference significantly smaller than the potential difference assigned to the magnetosphere, it dissipates in the ionosphere within 5-10 minutes, disproving the theory that movement of the magnetic flux can sustain magnetospheric convection when the electric current circuit connected to the ionosphere is taken into account.

2.3 Earth-Ionosphere Transmission Line (Polar Ionosphere-Equatorial Ionosphere)

The Poynting flux that propagates to the polar ionosphere penetrates into the ionosphere, whereupon a part of it is consumed by Joule dissipation. The remaining flux propagates as TM0 modes through the transmission lines constituted by Earth-ionosphere waveguides. Kikuchi et al. (1978) and Kikuchi and Araki (1979) have demonstrated that these transmission lines carry the polar electric field to low latitudes. The Poynting flux transferred in the horizontal (x -direction) by the TM0 mode is the product of the vertical electric field (E_z) and the magnetic field perpendicular to the plane of propagation (H_y). When the ionospheric conductance is sufficiently large, the electric field within the transmission line is nearly perpendicular to the ionosphere. The Poynting flux penetrating into the ionosphere, consisting of E_x and H_y , can be ignored. Therefore, the TM0 is subject only to geometrical attenuation (Kikuchi and Araki, 1979). On the other hand, the conductance is smaller in the nightside ionosphere than in the

dayside ionosphere by more than one order of magnitude. In this case, the electric field component parallel to the ionosphere, E_x , cannot be ignored. This means that there will be an influx of Poynting flux into the ionosphere of $E_x H_y$, attenuating the Poynting flux propagating in the x-direction.

When S is the Poynting flux propagating horizontally along the Earth-ionosphere waveguide, the value of S at distance x from the source electric field in the dayside polar ionosphere is expressed by $S(x) = A S(0)$. A is the transmission coefficient given by the following equation:

$$A = e^{-\frac{x}{h} \frac{\mu_0 V_a}{377(1 + \mu_0 V_a \sigma d)}} \quad (20)$$

Here, h is the ionospheric altitude, V_a the Alfvén velocity, σ the ionospheric conductivity, and d the thickness of the ionosphere. When $V_a = 1,000$ km/s, $x = 5,000$ km, $h = 100$ km, $\sigma d = 0.2-10$ mho, the transmission coefficient is:

$$A = 0.875-0.988. \quad (21)$$

The ionospheric conductance on the day-side is 5-10 mho. On the nightside, it is 1 mho or less. Therefore, the conductance of 0.2 mho is lower than values normally considered for the nightside ionosphere. But even in this case, the transmission coefficient is 0.875 ; the attenuation during propagation of the TM0 mode is negligible.

In models that include the MHD medium

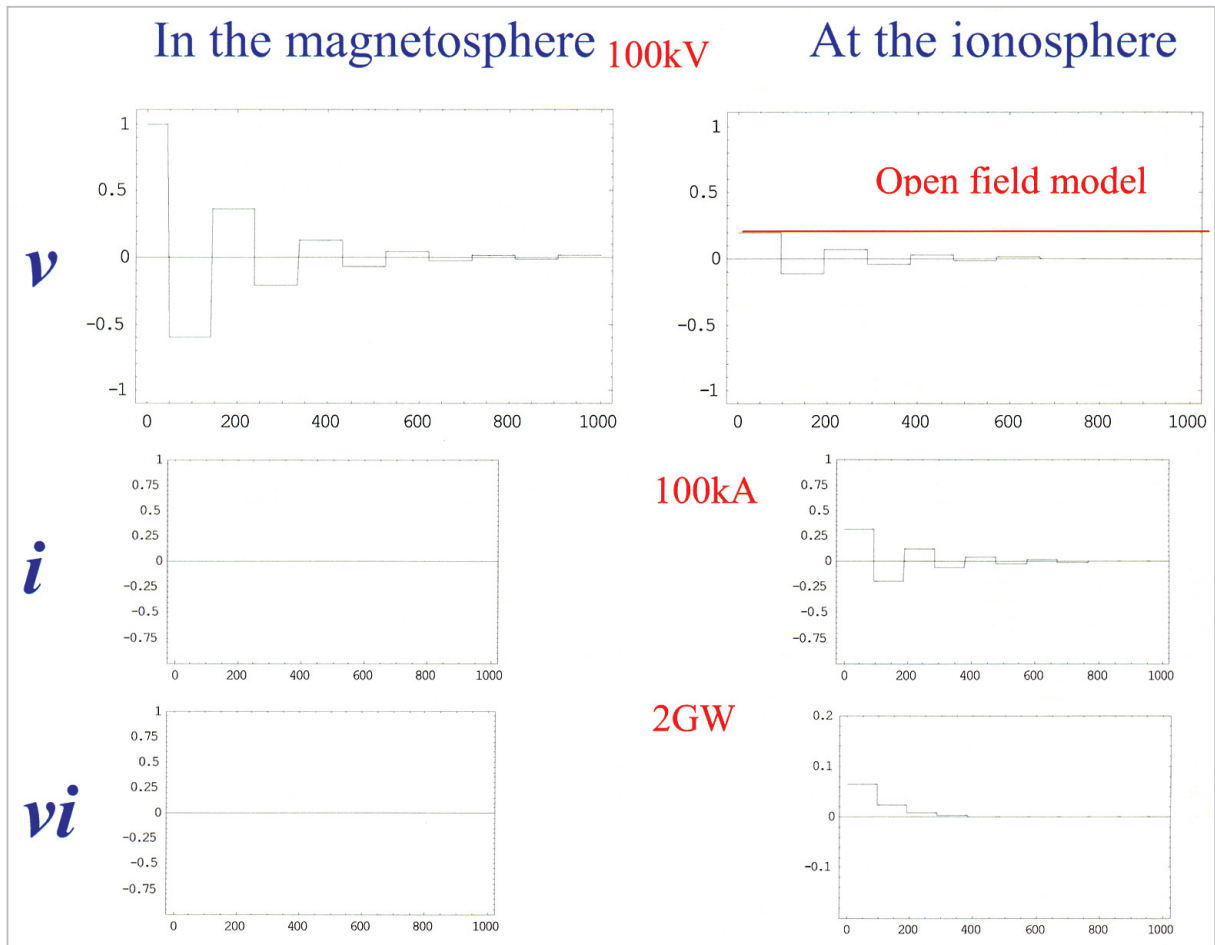


Fig. 16 The electric potential (upper left), current (middle left), and energy (lower left) at the generator, and the electric potential (upper right), current (middle right), and energy (lower right) at the ionosphere, assuming infinite internal resistance for the generator and a given initial electric potential for the transmission line in the magnetosphere-ionosphere transmission line model.

See Fig.15 for the parameters of the transmission line and ionosphere and units for the vertical axis.

(F region, inner magnetosphere) above the ionosphere, a part of the Poynting flux that penetrates from the vacuum into the ionosphere is lost in the conductive ionosphere (E region) due to Joule dissipation; but a part of the flux manages to propagate into the above MHD region as Alfvén waves. The ratio of the energies that are lost and transmitted is determined by the ratio of ionospheric conductance to the Alfvén conductance (Kikuchi and Araki, 1979). On the dayside, where the ionospheric conductance is larger than the Alfvén conductance, most of the energy is consumed in the E region by Joule dissipation. The electric field determined by the ionospheric current and the ionospheric conductance penetrates into the MHD medium along magnetic field lines.

In contrast, when the ionospheric conductance is small, the effect of Joule dissipation is also small, and the magnetic field component of the TM₀ mode propagates into the MHD region, releasing substantial energy into the inner magnetosphere as Alfvén waves. The electric field in this case is the magnetic field component divided by the Alfvén conductance.

2.4 Open Transmission Lines (Ionospheric generator-inner magnetosphere)

The detailed discussion in the previous section of the energy transfer from the ionosphere to the inner magnetosphere notwithstanding, determining the electric potential of the inner magnetosphere requires further study of ionosphere-magnetosphere interactions by applying the transmission line model. For this purpose, the generator is assumed to exist in the ionosphere, and the transmission line model with the ionospheric conductance as the internal resistance is applied.

If the northern and southern hemispheres are assumed to be symmetrical, the current at the magnetic equator corresponding to the load is zero, and the transmission lines are open. Fig.17 presents a case for the above relational expression for the condition of $R = \infty$ and a small nightside ionospheric conductance

(ionospheric conductance < Alfvén conductance). The left and right panels at the top of Fig.17 show the temporal variations in potential difference at the magnetospheric equatorial plane and the ionosphere, respectively.

Since the characteristic conductance of the transmission lines is higher than the internal conductance of the generator, the electric potential difference does not display a step-wise increase, but achieves a steady state after some relaxation time. The major difference from the case of the magnetospheric generator is the small difference between the potential differences of the ionosphere and the magnetosphere, which indicates that the ionospheric plasma and the magnetospheric plasma are moving as a unit. The current and energy escape from the ionosphere only when the potential difference is increasing; no energy is consumed in the steady state. These results show that when an electric potential is assigned to the ionosphere, the ionospheric plasma and the magnetospheric plasma both begin to move simultaneously. After a certain relaxation time, both achieve a steady pattern of motion (convection). This relaxation time may correspond to the 5-10 minute lag from the development of the polar cap potential to the initiation of the magnetospheric partial ring current (Hashimoto et al., 2002).

3 Conclusions

As shown in this paper, many of the magnetic disturbances observed on the ground can be explained by a 3-D current system composed of a magnetospheric current generator, FACs, and ionospheric currents. The magnetic disturbances due to ionospheric currents at high latitudes are caused mainly by Hall currents, while the prominent magnetic disturbance at the dayside magnetic equator is caused mainly by Pedersen currents intensified by the Cowling effect. The direct magnetic field effect of FACs also plays an important role at mid-latitudes.

Since the ionospheric Pedersen current accompanies energy loss, electromagnetic

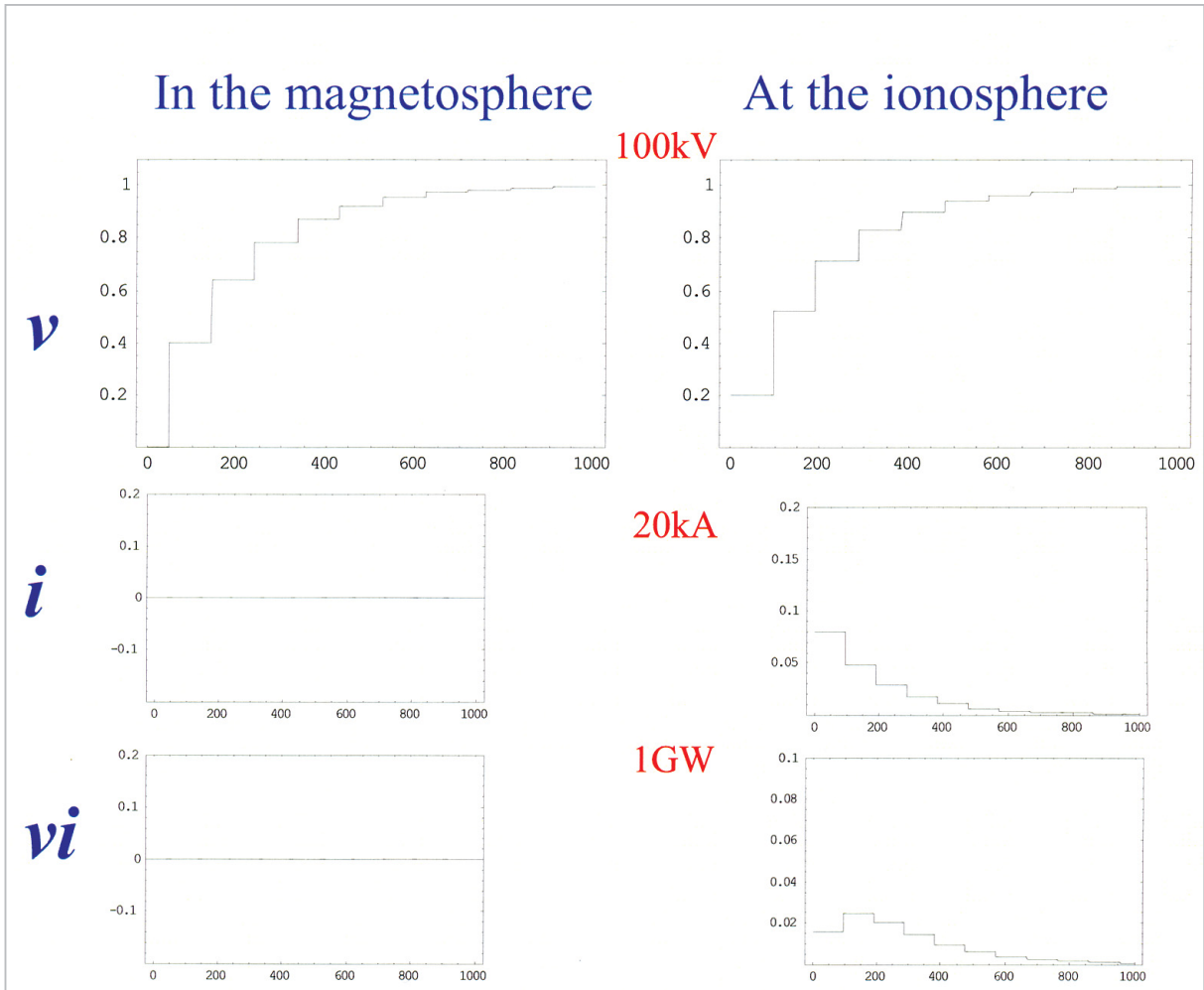


Fig. 17 The electric potential (upper left), current (middle left), and energy (lower left) at the generator, and the electric potential (upper right), current (middle right), and energy (lower right) at the ionosphere, assuming that the generator exists in the ionosphere, with the ionospheric conductance of 0.10 mho corresponding to the internal resistance, and assuming that $V_a = 2,000$ km/s, in the magnetosphere-ionosphere transmission line model.

energy (Poynting flux) must be supplied from the magnetosphere to sustain the 3-D current system. In the case of magnetospheric convection, the Poynting flux ejected from the generator near the cusp is transported to the polar ionosphere through the space between R1 FACs, which serve as transmission lines. In the polar ionosphere, part of the energy is lost due to the Pedersen current, but some is transported horizontally through the Earth-ionosphere waveguide to the nightside ionosphere and the mid-to-low latitude ionosphere. A part of the Poynting flux transported to low latitudes by the Earth-ionosphere waveguide penetrates into the MHD medium above, i.e., into the ionospheric F region, resulting in motions of the F-region plasma. This plasma motion

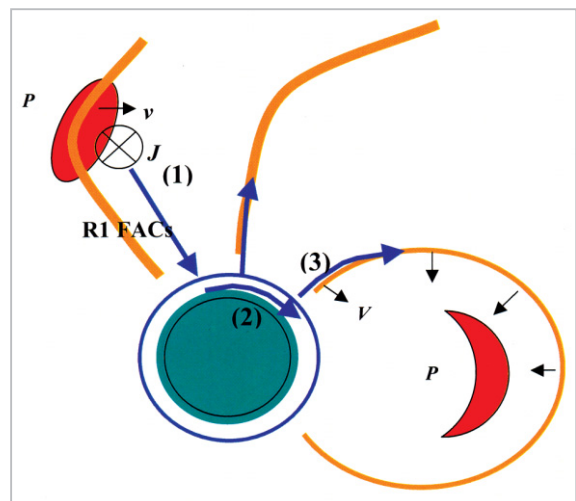


Fig. 18 The magnetosphere-ionosphere transmission line model.

The transmission line system is composed of the following 3 lines: (1) generator-ionosphere transmission line; (2) Earth-ionosphere waveguide; and (3) ionosphere-inner magnetosphere transmission line.

can be observed by the HF Doppler method. The Poynting flux transported to the nightside ionosphere is carried into the nightside inner magnetosphere via magnetospheric transmis-

sion lines and generates the partial ring current. The transfer of the Poynting flux between these regimes is illustrated schematically in Fig.18.

References

- 1 Araki, T., "Global structure of geomagnetic sudden commencements", *Planet. Space Sci.*, 25, 373-384, 1977.
- 2 Araki, T., "A physical model of the geomagnetic sudden commencement, Solar Wind Sources of Magnetospheric Ultra-Low-Frequency Waves", *Geophysical Monograph* 81, 183-200, 1994.
- 3 Chen, L. and A. Hasegawa, "A theory of long-period magnetic pulsations 1. Steady state excitation of field line resonance", *J. Geophys. Res.*, 89, 2765, 1974.
- 4 Clauer, C. R., and Y. Kamide, "DP1 and DP2 current systems for the March 22, 1979 substorms", *J. Geophys. Res.*, 90, 1343-1354, 1985.
- 5 Cowley, S. W. H. and M. Lockwood, "Excitation and decay of solar wind-driven flows in the magnetosphere system", *Ann. Geophysicae*, 10, 103-115, 1992.
- 6 Crooker, N. U., and G. L. Siscoe, "Birkeland currents as the cause of the low-latitude asymmetric disturbance field", *J. Geophys. Res.*, 86, 11201-11210, 1981.
- 7 Dungey, J.W., "Interplanetary magnetic field and the auroral zones", *Phys. Rev. Lett.*, 6, 47, 1961.
- 8 Fejer, B. G., D. T. Farley, B. B. Balsley, and R. F. Woodman, "Radar studies of anomalous velocity reversals in the equatorial ionosphere", *J. Geophys. Res.*, 81, 4621-4626, 1976.
- 9 Forbush, S. E., and E. H. Vestine, "Daytime enhancement of size of sudden commencements and initial phase of magnetic storms at Huancayo", *J. Geophys. Res.*, 60, 299-316, 1955.
- 10 Gonzales, C. A., M. C. Kelley, B. G. Fejer, J. F. Vickrey, and R. F. Woodman, "Equatorial electric fields during magnetically disturbed conditions 2. Implications of simultaneous auroral and equatorial measurements", *J. Geophys. Res.*, 84, 5803-5812, 1979.
- 11 Gonzales, C. A., M. C. Kelley, R. A. Behnke, J. F. Vickrey, R. Wand, and J. Holt, "On the latitudinal variations of the ionospheric electric field during magnetospheric disturbances", *J. Geophys. Res.*, 88, 9135-9144, 1983.
- 12 Gouin, P., "Reversal of the Magnetic daily variation at Addis Ababa", *Nature*, 1145-1146, 1962.
- 13 Hashimoto, K., T. Kikuchi, and Y. Ebihara, "Response of the magnetospheric convection to sudden IMF changes as deduced from the evolution of partial ring currents", *J. Geophys. Res.*, 107, 2002 in print.
- 14 Hirono, M., "A theory of diurnal magnetic variations in equatorial regions and conductivity of the ionosphere E region", *J. Geomag. Geoelectr.*, Kyoto, 4, 7-21, 1952.
- 15 Hutton, R., "The interpretation of surface equatorial magnetic daily variations on disturbed days", *Planet. Space Sci.*, 20, 1113-1116, 1972.
- 16 Iijima, T., and T. A. Potemra, "The amplitude distribution of field -aligned currents at northern high latitudes observed by Triad", *J. Geophys. Res.*, 81, 2165-2174, 1976.
- 17 Iijima, T., "Field-aligned currents in geospace: Substance and significance, Magnetospheric Current Systems", *Geophysical Monograph* 118, 107-129, 2000.
- 18 Kelley, M. C., B. G. Fejer, and C. A. Gonzales, "An explanation for anomalous equatorial ionospheric electric fields associated with a northward turning of the interplanetary magnetic field", *Geophys. Res. Lett.*, 6, 301-304, 1979.

- 19 Kikuchi, T., T. Araki, H. Maeda, and K. Maekawa, "Transmission of polar electric fields to the equator", *Nature*, 273, 650-651, 1978.
- 20 Kikuchi, T., and T. Araki, "Horizontal transmission of the polar electric field to the equator", *J. Atmosph. Terrest. Phys.*, 41, 927-936, 1979.
- 21 Kikuchi, T., T. Ishimine, and H. Sugiuchi, "Local time distribution of HF Doppler frequency deviations associated with storm sudden commencements", *J. Geophys. Res.*, 90, pp.4389-4393, 1985.
- 22 Kikuchi, T., and T. Araki. "Preliminary positive impulse of geomagnetic sudden commencement observed at dayside middle and low latitudes", *J. Geophys. Res.*, 90, 12195-12200, 1985.
- 23 Kikuchi, T., "Evidence of transmission of polar electric fields to the low latitude at times of geomagnetic sudden commencements", *J. Geophys. Res.*, 91, 3101-3105, 1986.
- 24 Kikuchi, T., H. Lühr, T. Kitamura, O. Saka, and K. Schlegel, "Direct penetration of the polar electric field to the equator during a DP 2 event as detected by the auroral and equatorial magnetometer chains and the EISCAT radar", *J. Geophys. Res.*, 101, 17161-17173, 1996.
- 25 Kikuchi, T., M. Pinnock, A. Rodger, H. Lühr, T. Kitamura, H. Tachihara, M. Watanabe, N. Sato, and M. Ruohoniemi, "Global evolution of a substorm-associated DP 2 current system observed by SuperDARN and magnetometers", *Advances in Space Research*, (in press), 2000a.
- 26 Kikuchi, T., H. Luehr, K. Schlegel, H. Tachihara, M. Shinohara, and T.-I. Kitamura, "Penetration of auroral electric fields to the equator during a substorm", *J. Geophys. Res.*, 105, 23,251-23,261, 2000b.
- 27 Kikuchi, T., S. Tsunomura, K. Hashimoto, and K. Nozaki, "Field-aligned current effects on midlatitude geomagnetic sudden commencements", *J. Geophys. Res.*, 106, pp. 15,555-15,565, 2001.
- 28 Kikuchi, T., B. Fejer, K. Hashimoto, T.-I. Kitamura and H. Tachihara, "Equatorial counter-electrojet during substorms", submitted, to *J. Geophys. Res.*
- 29 Kivelson, M. G. and D. J. Southwood, "Resonant ULF waves: A new interpretation", *Geophys. Res. Lett.*, 12, 49, 1985.
- 30 Matsushita, S., "On geomagnetic sudden commencements, sudden impulses, and storm durations", *J. Geophys. Res.*, 67, 3753-3777, 1962.
- 31 Motoba, T., T. Kikuchi, H. Lühr, H. Tachihara, T.-I. Kitamura, K. Hayashi, and T. Okuzawa, "Global Pc 5 caused by a DP 2-type ionospheric current system", *J. Geophys. Res.*, 107, SMP7-1, 2002.
- 32 Nagata, T., "Distribution of SC* of magnetic storms", *Rep. Ionosph. Res. Japan*, 6, 13-30, 1952.
- 33 Nishida, A., N. Iwasaki, and T. Nagata, "The origin of fluctuations in the equatorial electrojet; A new type of geomagnetic variation", *Annales Geophysicae*, 22, 478-484, 1966.
- 34 Nishida, A., "Coherence of geomagnetic DP2 magnetic fluctuations with interplanetary magnetic variations", *J. Geophys. Res.*, 73, 5549-5559, 1968.
- 35 Obayashi, T., and J. A. Jacobs, "Sudden commencements of magnetic storms and atmospheric dynamo action", *J. Geophys. Res.*, 62, 589-616, 1957.
- 36 Rastogi, R. G., and N. S. Sastri, "On the occurrence of SSC(-+) at geomagnetic observatories in India", *J. Geomag. Geoelectr.*, 26, 529-537, 1974.
- 37 Reddy, C. A., S. Ravindran, K. S. Viswanathan, B. V. Krishna Murthy, D. R. K. Rao, and T. Araki, "Observation of Pc 5 micropulsation related electric field oscillations in the equatorial ionosphere", *Ann. Geophys.*, 12, 565, 1994.
- 38 Samson, J. C., J. A. Jacobs, and G. Rostoker, "Latitude dependent characteristics of long-period geomagnetic micropulsations", *J. Geophys. Res.*, 76, 3675, 1971.
- 39 Samson, J. C. and G. Rostoker, "Latitude-dependent characteristics of high latitude Pc 4 and Pc 5 micropulsations", *J. Geophys. Res.*, 77, 6133, 1972.

-
- 40 Sugiura, M., "The solar diurnal variation in the amplitude of sudden commencements of magnetic storms at the geomagnetic equator", J. Geophys. Res., 58, 558-559, 1953.
- 41 Tanaka, T., "Generation mechanisms for magnetosphere-ionosphere current systems deduced from a three-dimensional MHD simulation of the solar wind-magnetosphere-ionosphere coupling processes", J. Geophys. Res., 100, 12057-12074, 1995.
- 42 Tamao, T., "Hydromagnetic interpretation of geomagnetic SSC* ", Rep. Ionos. Space Res. Japan, 18, 16-31, 1964.
- 43 Trivedi, N. B., B. R. Arora, A. L. Padilha, J. M. Da Costa, S. L. G. Dutra, F. H. Chamalaun, and A. Rigoti, "Global Pc 5 geomagnetic pulsations of March 24, 1991, as observed along the American sector", Geophys. Res. Lett., 24, 1683, 1997.
- 44 Vasyliunas, V. M., "The interrelationship of magnetospheric processes, Earth's Magnetospheric Processes", ed. B. M. McCormac, 29-38, 1972.
- 45 Ziesolleck, C. W. S. and F. H. Chamalaun, "A two dimensional array study of low-latitude Pc5 geomagnetic pulsations", J. Geophys. Res., 98, 13705, 1993.



KIKUCHI Takashi, Ph. D.
*Research Supervisor, Applied Research
and Standards Division
Magnetosphere-Ionosphere Physics*